Korean J. Chem. Eng., 40(3), 519-523 (2023)
DOI: 10.1007/s11814-022-1304-z

pISSN: 0256-1115
eISSN: 1975-7220

Degradation mechanism of polyethylene separators in lithium-ion batteries after prolonged cycling

Ye Ji Ha*, Yun Jeong Choi, Jeong-In Choi**, Bo Keun Park*, Jin Hyuk Yang*, and Ki Jae Kim*,†**

*Department of Energy Science, Sungkyunkwan University, Suwon, Gyeonggi-do 16419, Korea
**Department of Energy Engineering, Konkuk University, Neungdong-ro 120, Gwangjin-gu, Seoul 05029, Korea
(*Received 22 August 2022 • Revised 22 September 2022 • Accepted 29 September 2022*)

Abstract−The degradation of lithium-ion batteries (LIBs) is caused by a complicated mechanism; therefore, identifying their degradation mechanism remains challenging. Most studies related to the degradation mechanism of LIBs have focused on the degradation of cathode and anode materials. A separator that provides a pathway for Li^+ ions is crucial for good electrochemical performance and safety of LIBs, but its degradation mechanism has rarely been studied. This study analyzed the relationship between the structural deformation of an aged separator and the electrochemical performance of LIBs. We discovered that even if the polyethylene (PE) separator is exposed to prolonged cycling under normal charging and discharging conditions, the by-products formed via electrolyte decomposition are firmly trapped in its pore, resulting in pore clogging. Additionally, the PE polymer chain gradually oxidizes at the part that is in contact with the cathode side, resulting in the loss of elasticity and breaking the polymer chain in the PE separator. These degradation processes of the PE separator can cause poor Li^+ ion conductivity throughout the aged separator, which eventually results in lower electrochemical performance, particularly the rate performance, of LIBs.

Keywords: Polyethylene Separator, Lithium-ion Batteries, Prolonged Cycling, Lithium-ion Battery Degradation, Lithium-ion Electrochemical Performance

INTRODUCTION

Lithium-ion batteries (LIBs) have been extensively used as power sources in various applications, ranging from portable devices to energy storage systems owing to their advantageous properties, such as high energy density, long cycle life, and low self-discharge [1,2]. Therefore, LIBs are globally employed as core devices in several electronics, and significant efforts are being devoted to the development of new materials to improve their performance [3-8]. To effectively enhance the performance of LIBs, the degradation mechanism of the materials employed in LIBs must be understood. However, identifying the degradation mechanism of LIBs remains challenging because of their complexity.

The performance degradation of LIBs originates from the complex interplay between different components, such as the cathode, anode, and separator [9-11]. Several researchers have reported the degradation mechanisms of the cathode and anode materials, such as particle cracking in the active material [12-14], lithium plating [15], and the formation and growth of unstable solid electrolyte interphases (SEIs) [16-18]. Although the separator, which prevents physical contact between the positive and negative electrodes, is a key component in achieving good electrochemical performance and safety of LIBs, its degradation mechanism has rarely been studied.

The separator is situated between the positive and negative electrodes, and it not only prevents an electrical short circuit but also allows the exchange of lithium ions through the liquid electrolyte to complete the circuit [19,20]. During prolonged cycling under charge-discharge conditions, the electrolyte decomposes [21], and the resulting products gradually accumulate on the separator and cause partial blocking of its pores, thereby decreasing both the pore size and separator homogeneity [22,23]. These factors increase the average path length for the Li ions and consequently decrease the ionic conductivity within the battery, which negatively impacts its electrochemical performance [24,25]. Therefore, it is necessary to identify the degradation mechanism of the separator and investigate the effect of an aged separator on the electrochemical performance of LIBs during battery operation.

Herein, we focused on analyzing the deterioration behavior of polyethylene (PE) separators that underwent prolonged cycling and subsequently demonstrated the effect of aged separators on the electrochemical performance of LIBs. For this purpose, a pouch-type LIB with a capacity of 75 Ah was prepared and galvanostatically charged and discharged between 2.5 and 4.3 V vs. Li/Li^+ at a constant current of 1C at room temperature. After the pouch cell reached its end of life (EOL), the aged separator was extracted by disassembling it. The physicochemical changes in the aged separator were thoroughly analyzed using scanning electron microscopy (SEM), energy dispersive X-ray spectroscopy (EDS), and Fourier transform infrared (FTIR) spectroscopy. Additionally, the effect of the change in the physicochemical properties of the aged separators on the battery performance was thoroughly investigated via cycling and rate capability tests of coin cells using the aged separators.

†To whom correspondence should be addressed.
E-mail: kijaekim@konkuk.ac.kr

EXPERIMENTAL

1. Preparation of Separator Samples

The batteries used in this study were large-format pouch-type LIBs with a nominal capacity of 75 Ah. The cells were cycled at 1C charge and 1C discharge rates under a controlled temperature of 25 °C (denoted as 1C/1C cell). The upper and lower cutoff voltages were set to 4.3 and 2.5 V. The positive and negative electrodes were $LiNi_{0.3}Co_{0.3}Mn_{0.3}O_2$ and graphite, respectively. To analyze the deterioration behavior of the PE separator equipped in LIBs, a pouch cell near its EOL, that is, when its capacity reached 80% of its initial capacity, was disassembled after full discharge. The obtained separators were washed twice with dimethyl carbonate (DMC) to remove any residue.

2. Characterization of Separators

To observe the microstructural changes, the surface morphology of the separators was investigated via field-emission SEM (FE-SEM, JSM 7000F, JEOL Company). The elemental composition of the sample surface was measured via EDS. FTIR spectroscopy (VERTEX 70, Bucker Company) was used to confirm the changes in the chemical functional groups of the separators. To determine the pore structure, air permeability was evaluated using a Gurley densometer (Toyoseiki) by measuring the time (s) required for 100 cm^3 of air to pass through the membrane of the separator.

3. Electrochemical Analyses of Separators

The ionic conductivity (σ) of the separators was measured via electrochemical impedance spectroscopy. Separators soaked in the electrolyte were sandwiched between two stainless steel electrodes over a frequency range of 0.1 Hz-1 MHz with an alternating current (AC) amplitude of 5 mV. The ionic conductivity was then calculated using the following equation: σ=I/RS, where I is the thickness of the separator; S is the effective contact area between the separator and stainless steel electrodes, and R is the bulk resistance of the wet separator. R was measured by AC complex impedance analysis (VSP, Biologic). To evaluate the electrochemical performance of the separators, lithium cobalt oxide electrodes were used to assemble half cells in a coin cell format with a Li anode, polyethylene separator, and 1 M lithium hexafluorophosphate ($LiPF_6$) in ethylene carbonate/ethyl methyl carbonate (EC/EMC, 3 : 7 v/v, Dongwha Electrolyte, South Korea) as the electrolyte. The cells were charged using constant current-constant voltage (CC-CV) and discharged using constant current (CC) within a voltage range of 3-4.3 V vs. Li/Li^+. In the first three cycles, the cells were charged and discharged at a rate of C/10. Their rate capability was evaluated by varying both the charging (operated in the CC-CV mode) and discharging current rate (operated in the CC mode) as follows: (C/5→C/2→1C→2C→3C→4C→5C).

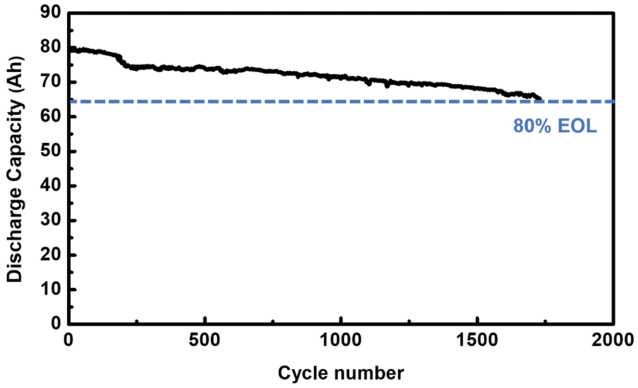

Fig. 1. Cycle life of the 1C/1C cell. Blue line indicates EOL.

RESULTS AND DISCUSSION

To analyze the degradation of the polyethylene separator after prolonged cycling, pouch-type LIBs with a capacity of 75 Ah were prepared and galvanostatically charged and discharged between 2.5 and 4.3 V vs. Li/Li^+ with a constant current of 1C at room temperature. As shown in Fig. 1, the discharge capacity of the battery gradually decreased, and it eventually reached its EOL at 1730 cycles (EOL is defined as the capacity reaching 80% of its initial capacity

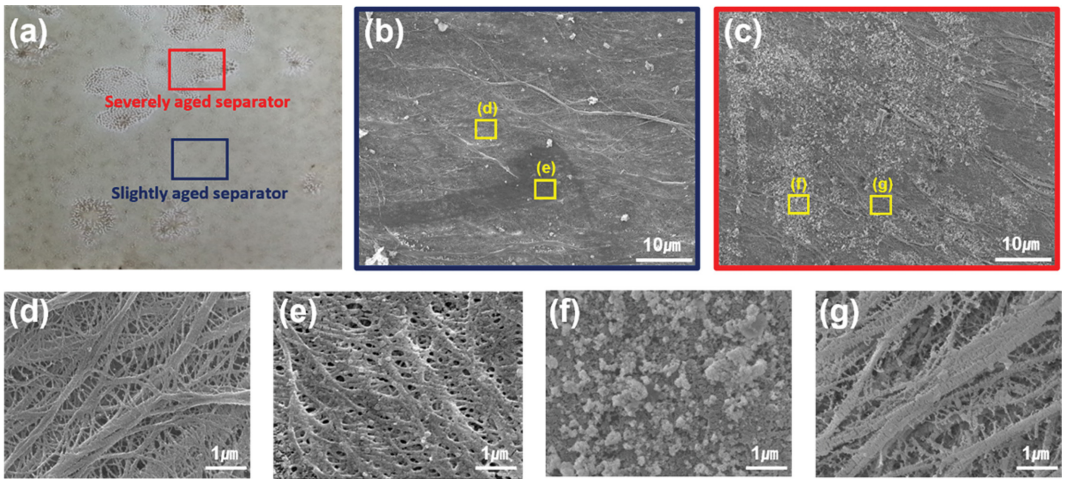

Fig. 2. (a) Highly magnified optical image of the aged separator. Severely and slightly damaged parts of the separator are indicated by blue and red squares, respectively. Low magnification micrographs of (b) slightly aged and (c) severely aged separators. SEM images of (d)-(e) slightly aged and (f)-(g) severely aged separators.

Table 1. EDS analysis results of the areas shown in Fig. 2

Element (wt%)	Position			
	d	e	f	g
C	100	95.84	79.21	91.35
O	0.00	2.49	8.30	5.15
F	0.00	1.42	8.95	1.26
P	0.00	0.16	2.68	1.46

in the Experimental section). The aged separator was extracted by disassembling the 1C/1C cell and was then washed with DMC to remove the electrolyte salts.

Optical and SEM images of the pristine PE and aged separators are shown in Fig. S1. For the pristine PE separator, a typical microstructure and white color without any degradation can be observed, whereas in the aged separator images, a faded brown color and an uneven deposition of by-products caused by electrolyte decomposition can be observed. As shown in Fig. 2(a), the high-magnification optical image of the aged separator can be divided into two parts: severely damaged and slightly damaged. To discern the microstructural changes based on the degree of damage, the surface morphology of each separator was explored using SEM. As shown in the SEM images in Fig. S1(c) and (d), typical microstructures with interconnected and elliptical pores can be observed in the pristine PE separator [26]. In contrast, as shown in Fig. 2(b) and (c), differences in the microstructures of the pristine PE and aged separators are clearly visible. In the severely aged separator (Fig. 2(f)), a region that is fully covered by the by-products is observed. EDS analysis was performed to investigate the chemical compositions of the by-products; the results are presented in Table 1. EDS analysis revealed that the oxygen, fluoride, and phosphorus content in the severely aged separator was 8.30, 8.95, and 2.68 wt%, respectively, indicating that these by-products resulted from the decomposition of the electrolyte and lithium salt on the electrode, which leads to SEI formation on the electrode surface [16,27]. Significantly, as shown in Fig. 2(g), several broken chains of PE separators can be clearly observed in the severely aged separator. This observation is in good agreement with the previously reported result that the PE separator becomes fragile owing to loss in elasticity after being affected by an oxidizing environment [28,29]. In contrast, the slightly aged separator underwent negligible degradation compared to the severely aged separator, as shown in Fig. 2(b). Specifically, certain parts of the slightly aged separator showed no damage (Fig. 2(d)), whereas several others showed a decreased pore size owing to the thickened fibrils caused by the by-products accumulated on the separators (Fig. 2(e)) [23]. Based on these observations, the severely aged separator was more deteriorated than the slightly aged separator.

During prolonged cycling, the cathode side of the separator encounters a severely oxidizing environment [30]. An oxidized PE separator loses its elasticity owing to the disintegration of PE molecular chains when it is subjected to strong oxidation, resulting in a decrease in its mechanical strength and a subsequent increase in the internal short probability [29]. Because it was exposed to oxidizing conditions for prolonged cycling, the surface chemistry of the aged separator was probably altered. To identify the changes in the surface chemistry of the aged separator, the aged and pristine separators were analyzed via FTIR spectroscopy. As shown in Fig. 3, the peaks corresponding to the CH stretching vibrations at 3,000-2,850 cm^{-1} and CH bending vibrations at 1,465 and 714 cm^{-1}, which are typical characteristic peaks of the PE separator, are observed in all separators [31]. Notably, significant signals corresponding to the carbonyl bond (1,750-1,720 cm^{-1}), CO bond stretching (1,124-1,087 cm^{-1}) and CH_3 bond bending (1,300 cm^{-1}) were observed in the FTIR spectra of the severely and slightly aged separators [32]. This is mainly attributed to the breaking of the hydrogen bonding (CH) chains in the PE separator owing to the continuous exposure to harsh oxidizing environments during prolonged cycling.

The results of this study clearly indicate that the microstructure and surface chemistry of the PE separator are altered by prolonged cycling, even during normal charge and discharge. To study the effect of these changes in the physicochemical properties of the PE

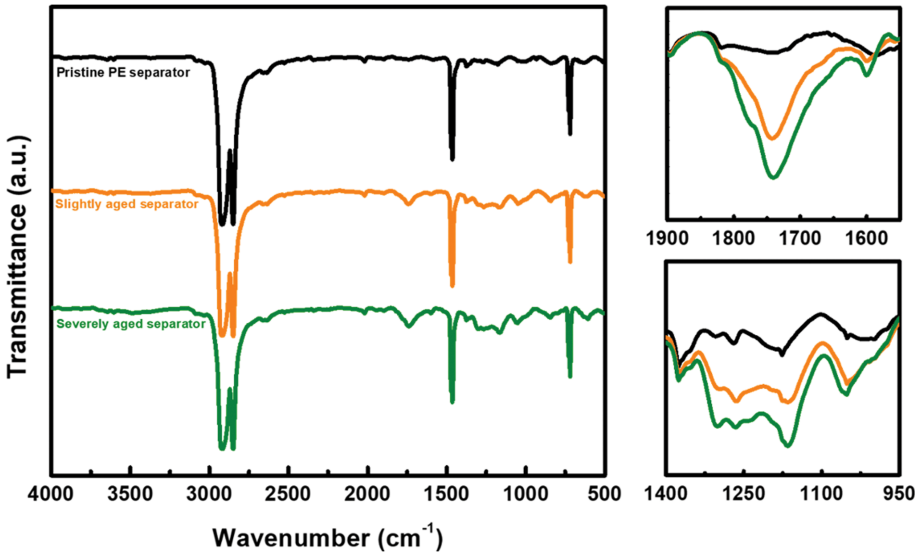

Fig. 3. FTIR spectra of the slightly aged (orange), severely aged (olive), and pristine PE separators (black).

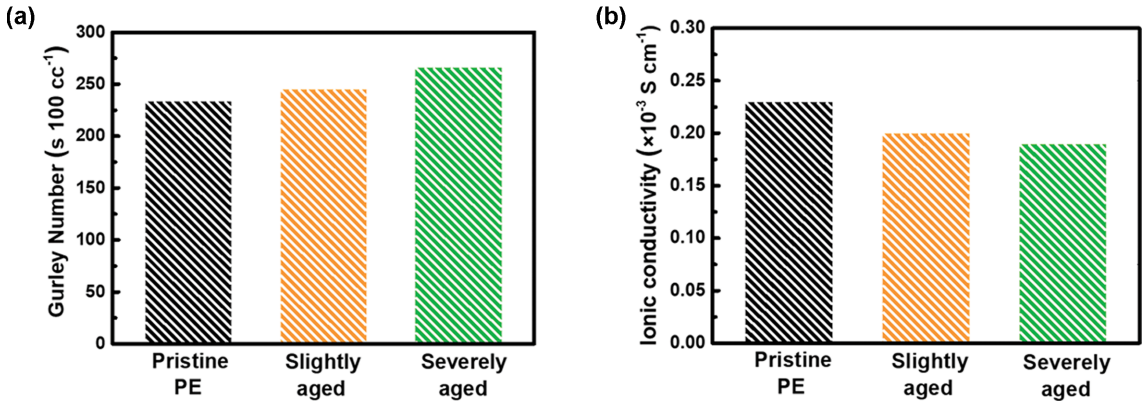

Fig. 4. (a) Gurley numbers and (b) ionic conductivity of the pristine PE, slightly aged, and severely aged separators.

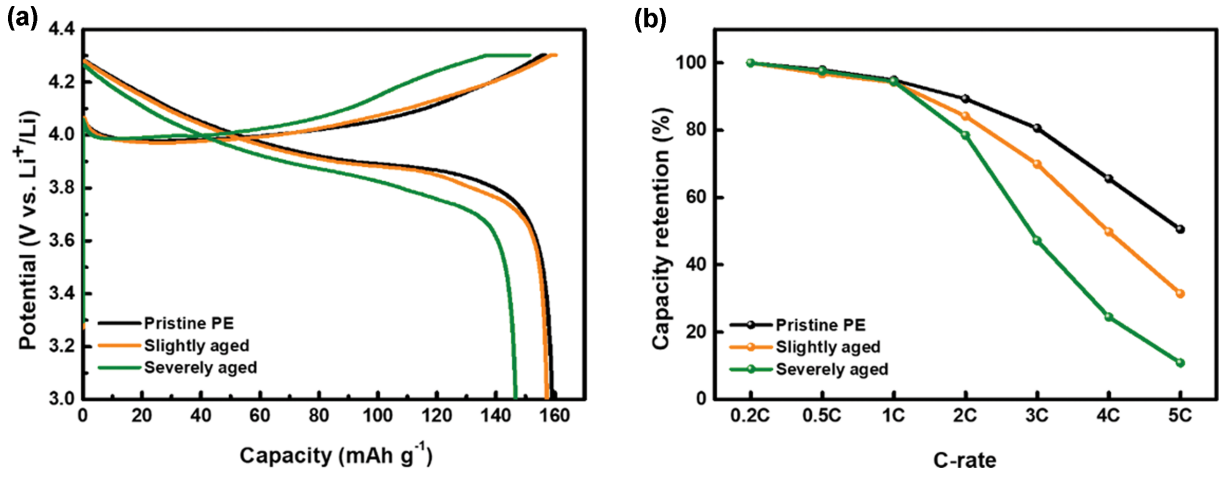

Fig. 5. (a) Initial charge/discharge profiles at 0.1C and (b) relative discharge capacity retention at different C-rates of the cells with the pristine PE, slightly aged, and severely aged separators.

separator on Li transport, the most well-known parameters related to Li transport, air permeability and ionic conductivity, were measured [33]. As shown in Fig. 4(a), the Gurley numbers of the severely and slightly aged separators were 266 and 245 s/100 cc, respectively, which were higher than that of the pristine PE separator (234 s/100 cc). Additionally, the ionic conductivity of the pristine and aged separators was measured; the results are shown in Fig. 4(b). The ionic conductivity of the slightly and severely aged separators was 0.20×10^{-3} and 0.19×10^{-3} S cm^{-1}, respectively, slightly lower than that of the pristine PE separator (0.23×10^{-3} S cm^{-1}). The poor air permeability and ionic conductivity of the aged separator are caused by the partial deposition of by-products on the fibrils, which diminishes the pore size and separator homogeneity, thereby increasing the average path length for the ions.

To understand the effects of the change in the physicochemical properties of the aged separators on the electrochemical performance of the battery, half-cells composed of $LiCoO_2$ cathodes, Li metal anodes, and slightly or severely aged separators were prepared, and their cycling and rate capability were tested. For comparison, half-cells composed of the same electrodes and pristine PE separators were also prepared. As shown in Fig. 5(a), the voltage profile of the cell with the slightly aged separator is similar to that of the cell with the pristine PE separator, and the cell with the slightly aged separator exhibits a discharge capacity of 160 mAh g^{-1}, which is approximately the same as that of the cell with the pristine PE separator. In contrast, the cell with the severely aged separator exhibits a considerably smaller discharge capacity (147 mAh g^{-1}) than the cell with the PE separator. Fig. 5(b) shows the discharge capacity retention of the cells with the aged and pristine PE separators at current rates of 0.2, 0.5, 1, 2, 3, 4, and 5C. The cells with the aged separators, particularly those with the severely aged separator, show lower rate performances than the cell with the pristine PE separator. This low rate performance is primarily attributed to the changed physicochemical properties of the aged separators, such as poor air permeability and ionic conductivity [34,35].

Based on these results, we can elucidate the complete degradation mechanism of the separator owing to prolonged cycling. When the PE separator is exposed to oxidizing conditions during prolonged cycling, even during normal charging and discharging, the by-products resulting from the reaction between the electrolyte surface and anode accumulate inside the pores and eventually damage the pore structure of the separator. Additionally, broken polymer chains were observed at the cathode side of the separator owing to the continuous exposure to a harsh oxidizing atmosphere, result-

ing in a decrease in the mechanical strength of the PE separator. Therefore, Li-ion transport throughout the aged separator was partially blocked owing to both degradation processes, eventually resulting in poor ionic conductivity and electrochemical performance of the battery with the aged separator.

CONCLUSIONS

This study elucidated the degradation mechanism of PE separators that undergo prolonged cycling and, subsequently, the effects of aged separators on the electrochemical performance of LIBs. Based on the SEM, EDS, and FTIR results of the separators, microstructural changes in the aged separator, including pore clogging and broken polymer chains, have a negative effect on its basic properties, such as ionic conductivity and mechanical strength. Pore clogging is primarily due to the formation of by-products owing to the electrolyte decomposition that occurs at the anode side. Moreover, the polymer chains were broken because of exposure to a severe oxidizing environment at the cathode side. Both degradation processes can change the physicochemical properties of the aged separator, such as its pore structure and mechanical strength. Consequently, these changes negatively influence the electrochemical performance of LIBs, particularly their rate performance. Therefore, we believe that this study is not only beneficial for understanding the deterioration characteristics of separators but also provides practical data that can aid in the design of advanced separators for LIBs.

ACKNOWLEDGEMENTS

This work was supported by the Technology Innovation Program (2011379 and 20010095) funded by the Ministry of Trade, Industry & Energy (MOTIE. Korea).

SUPPORTING INFORMATION

Additional information as noted in the text. This information is available via the Internet at http://www.springer.com/chemistry/journal/11814.

REFERENCES

1. B. Dunn, H. Kamath and J. M. Tarascon, *Science*, **334**, 928 (2011).
2. B. K. Park, Y. K. Jeong, S. Y. Yang, S. Y. Kwon, J. H. Yang, Y. M. Kim and K. J. Kim, *J. Power Sources*, **506**, 230222 (2021).
3. M. Li, J. Lu, Z. Chen and K. Amine, *Adv. Mater.*, **30**, 33 (2018).
4. J. W. Choi and D. Aurbach, *Nat. Rev. Mater.*, **1**, 1 (2016).
5. H. Zhang, H. Zhao, M. A. Khan, W. Zou, J. Xu, L. Zhang and J. Zhang, *J. Mater. Chem. A.*, **6**, 20564 (2018).
6. G. Chen, L. Yan, H. Luo and S. Guo, *Adv. Mater.*, **28**, 7580 (2016).
7. H. Pan, S. Zhang, J. Chen, M. Gao, Y. Liu, T. Zhu and Y. Jiang, *Mol. Syst. Des. Eng.*, **3**, 748 (2018).
8. Y. Li, Q. Li and Z. Tan, *J. Power Sources*, **443**, 227262 (2019).
9. J. M. Reniers, G. Mulder and D. A. Howey, *J. Electrochem. Soc.*, **166**, A3189 (2019).
10. A. Barré, B. Deguilhem, S. Grolleau, M. Gérard, F. Suard and D. Riu, *J. Power Sources*, **241**, 680 (2013).
11. J. H. Kim, S. C. Woo, M. S. Park, K. J. Kim, T. E. Yim, J. S. Kim and Y. J. Kim, *J. Power Sources*, **229**, 190 (2013).
12. D. E. Demirocak and B. Bhushan, *J. Power Sources*, **280**, 256 (2015).
13. A. Mukhopadhyay and B. W. Sheldon, *Prog. Mater. Sci.*, **63**, 58 (2014).
14. Y. K. Ahn, Y. N. Jo, W. Cho, J. S. Yu and K. J. Kim, *Energies*, **12**, 1 (2019).
15. J. Cannarella and C. B. Arnold, *J. Electrochem. Soc.*, **162**, A1365 (2015).
16. J. H. Yang, S. J. Hwang, S. K. Chun and K. J. Kim, *J. Electrochem. Sci. Technol.*, **13**, 208 (2022).
17. S. Phul, A. Deshpande and B. Krishnamurthy, *Electrochim. Acta*, **164**, 281 (2015).
18. T. Yoshida, M. Takahashi, S. Morikawa, C. Ihara, H. Katsukawa, T. Shiratsuchi and J. Yamaki, *J. Electrochem. Soc.*, **153**, A576 (2006).
19. P. Arora and Z. Zhang, *Chem. Rev.*, **104**, 4419 (2004).
20. V. Deimede and C. Elmasides, *Energy Technol.*, **3**, 453 (2015).
21. B. S. Parimalam, A. D. MacIntosh, R. Kadam and B. L. Lucht, *J. Phys. Chem. C.*, **121**, 22733 (2017).
22. M. F. Lagadec, R. Zahn and V. Wood, *J. Electrochem. Soc.*, **165**, A1829 (2018).
23. R. Kostecki, L. Norin, X. Song and F. McLarnon, *J. Electrochem. Soc.*, **151**, A522 (2004).
24. M. F. Lagadec, R. Zahn and V. Wood, *Nat. Energy*, **4**, 16 (2019).
25. Y. Saito, W. Morimura, R. Kuratani and S. Nishikawa, *J. Phys. Chem. C.*, **120**, 3619 (2016).
26. H. Lee, M. Yanilmaz, O. Toprakci, K. Fu and X. Zhang, *Energy Environ. Sci.*, **7**, 3857 (2014).
27. Y. Zheng, Y. He, K. Qian, B. Li, X. Wang, J. Li, C. Miao and F. Kang, *J. Alloys Compd.*, **639**, 406 (2015).
28. A. F. Reano, A. Guinault, E. Richaud and B. Fayolle, *Polym. Degrad. Stab.*, **149**, 78 (2018).
29. W. Böhnstedt, *J. Power Sources*, **67**, 299 (1997).
30. D. Ren, X. Feng, L. Lu, M. Ouyang, S. Zheng, J. Li and X. He, *J. Power Sources*, **364**, 328 (2017).
31. K. J. Kim, Y. H. Kim, J. H. Song, Y. N. Jo, J. Kim and Y. Kim, *J. Power Sources*, **195**, 6075 (2010).
32. N. B. Colthup, L. H. Daly and S. E. Wiberley, *Introduction of infrared and raman spectroscopy*, Academic Press, New York (1990).
33. X. Huang, *J. Solid State Electrochem.*, **15**, 649 (2011).
34. D. Djian, F. Alloin, S. Martinet, H. Lignier and J. Y. Sanchez, *J. Power Sources*, **172**, 416 (2007).
35. R. Chandrasekaran, *J. Power Sources*, **262**, 501 (2014).

Supporting Information

Degradation mechanism of polyethylene separators in lithium-ion batteries after prolonged cycling

Ye Ji Ha, Yun Jeong Choi*, Jeong-In Choi*, Bo Keun Park, Jin Hyuk Yang, and Ki Jae Kim†

Department of Energy Science, Sungkyunkwan University, Suwon, Gyeonggi-do 16419, Korea
*Department of Energy Engineering, Konkuk University, Neungdong-ro 120, Gwangjin-gu, Seoul 05029, Korea
(*Received 22 August 2022 • Revised 22 September 2022 • Accepted 29 September 2022*)

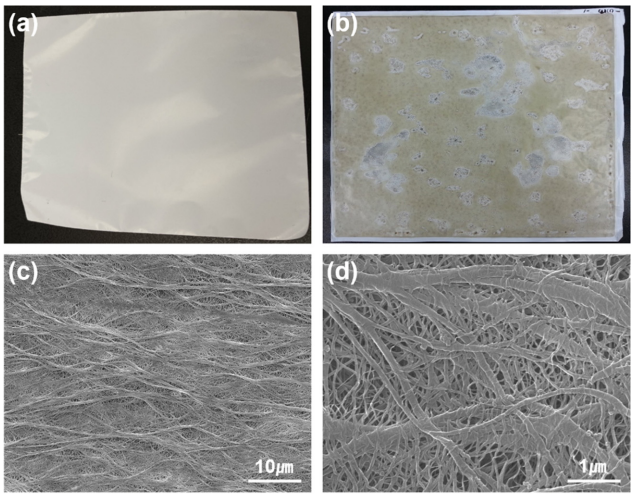

Fig. S1. The surface appearance of (a) the pristine PE separators and (b) the aged separator. (c) Low magnification micrographs and (d) high magnification micrographs of the pristine PE separator.